crystals

MDPI

Article

Impact of Synthesis Parameters on the Crystallinity of Macroscopic Zeolite Y Spheres Shaped Using Resin Hard Templates

Zahra Asgar Pour [1,*], Edrees Abu Zeitoun [2], Yasser A. Alassmy [3], Mustapha El Hariri El Nokab [4], Paul H. M. Van Steenberge [5] and Khaled O. Sebakhy [5,6,*]

1 Research and Development Department, Kisuma Chemicals, Billitonweg 7, 9641 KZ Veendam, The Netherlands
2 Chemistry Program, School of Arts and Sciences, American International University, Al Jahra 003200, Kuwait; e.zeitoun@aiu.edu.kw
3 King Abdulaziz City for Science and Technology (KACST), Riyadh 11442, Saudi Arabia; yalassmy@kacst.gov.sa
4 Department of Chemistry, Michigan State University, East Lansing, MI 48824, USA; elhariri@msu.edu
5 Laboratory for Chemical Technology (LCT), Department of Materials, Textiles and Chemical Engineering, Ghent University, Technologiepark 125, B-9052 Ghent, Belgium; paul.vansteenberge@ugent.be
6 Centre for Polymer and Material Technologies (CPMT), Ghent University, Technologiepark 130 (Zone C3), Zwijnaarde, B-9052 Ghent, Belgium
* Correspondence: asgarpour@kisuma.com (Z.A.P.); khaled.sebakhy@ugent.be (K.O.S.)

Abstract: In this study, the effects of several synthesis parameters including aging time, micropore-structure-directing agents, and hydrothermal treatment temperature profile were systematically examined with respect to their impact on the crystallinity of macroscopic zeolite Y spheres formed in the presence of organic anion-exchange resin templates. Spherical resins were utilized as hard templates to shape the zeolite Y particles. Zeolite Y precursors were initially deposited into the pores of the resin template and subsequently crystallized over time through precise control over these synthesis parameters. The resulting zeolite Y spheres were characterized using an array of characterization techniques, including XRD, SEM, TEM, BET, FTIR, and XRF. We identify the optimal conditions for maximizing the crystallinity of the macroscopic zeolite Y particles using resin templates as macroscopic shaping agents. This functional material has the potential to be used as both catalyst and adsorbent in several applications.

Keywords: crystallization; macroscopic zeolite Y spheres; hard templating technique; resin template; zeolite shaping; inorganic crystallization; morphological changes

Citation: Asgar Pour, Z.; Abu Zeitoun, E.; Alassmy, Y.A.; El Hariri El Nokab, M.; Van Steenberge, P.H.M.; Sebakhy, K.O. Impact of Synthesis Parameters on the Crystallinity of Macroscopic Zeolite Y Spheres Shaped Using Resin Hard Templates. *Crystals* **2024**, *14*, 1051. https://doi.org/10.3390/cryst14121051

Academic Editor: Eamor M. Woo

Received: 17 October 2024
Revised: 25 November 2024
Accepted: 27 November 2024
Published: 2 December 2024

1. Introduction

Over the past decades, there has been significant interest in the application of zeolites, ranging from catalysis and adsorption to advanced technologies such as gas storage, membranes, and composite materials [1,2]. While the high surface area of zeolites, attributed to their microporous structure (pore diameter < 1.5 nm) extended throughout a crystalline framework, is a crucial feature, it alone is insufficient to guarantee optimal performance in various applications. The active sites within the zeolite's micropores must be efficiently accessible to molecules in contact with gas or liquid phases [3]. In particular, when the interacting species are significantly larger than the zeolite's pore size, enhancing mass transfer and minimizing diffusion limitations necessitates the introduction of larger secondary pores, such as mesopores (2 nm < pore diameter < 50 nm) and macropores (pore diameter > 50 nm), into the microporous structure [4]. A porous zeolite framework containing these larger meso- and macropores, interconnected with intrinsic micropores, is referred to as hierarchical zeolites [5].

Various methods for synthesizing hierarchical zeolites have been explored over the last two decades [6,7]. In this study, a hard templating technique was employed using spherical resin templates to introduce hierarchical porosity into the microporous network of zeolite Y, which also facilitated the simultaneous formation of zeolite spheres. This approach eliminates the need for conventional shaping techniques that involve binder materials such as clays or inorganic oxides, which can alter the physicochemical properties of zeolites adversely; thus, it serves as an alternative to the extrusion technique [8]. However, the crystallization of the primary precipitated phase on a surface, such as a porous polymeric material, is challenging and differs from the zeolite bulk formation in powder form [9,10].

To maximize the crystallinity of zeolite Y in the presence of resin beads, we systematically investigated the effects of various synthesis parameters. By precisely adjusting these parameters and removing the organic resin via calcination, zeolite Y spheres with diameters ranging from 0.5 to 0.8 mm were successfully obtained. The use of resin templates has previously been reported for shaping other zeolitic frameworks, such as silicalite-1, ZSM-5, and zeolite Beta [11–13]. In our prior work, we reported the synthesis of zeolite Y beads with high crystallinity; however, the effects of varying synthesis parameters were not discussed [14]. The resin template used in this study (Amberlite IRA-900-Cl^-) is a copolymer of styrene-divinylbenzene with a spherical geometry and a porous macroreticular structure [15]. The presence of Cl^- anions in the functional groups of the resin particles imparts ion-exchange properties, which facilitate the deposition of zeolite precursors from the suspension into the pores of the resin over time. However, optimizing the synthesis parameters is essential for transforming the initial amorphous phase into a fully crystalline zeolitic phase [14]. Furthermore, the formation of zeolitic crystallites within the polymeric matrix is influenced by the restricted growth rate due to the confinement effects within the resin's pores, as well as the chemistry of the resin itself. From a textural perspective, the porous structure of the spherical zeolite particles mirrors the porous pattern of the resin template.

This work details how synthesis parameters, such as aging time, hydrothermal treatment temperature, and the use of organic structure-directing agents, were tailored to achieve zeolite Y crystallization within the resin template. Additionally, this method can be extended for shaping other low Si/Al ratio zeolites.

1. This study highlights the importance of shaping for functional materials (i.e., catalysts and adsorbents) in industrial-scale applications, because these materials in powder form impose a pressure drop in catalytic reactors and process units. In addition, efficient shaping including appropriate geometry of the final body as well as textural properties like porosity can directly impact the process parameters such as reactor size. However, shaping in most cases needs utilization of a binder (e.g., inorganic oxides like silica or alumina or mineral clays like kaolin) which can adversely impact the physicochemical properties of the functional material. To address these disadvantages, our developed hard-templating technique preserves the original physicochemical properties of zeolite because no extra additives like binders are used during the synthesis. This could be further explained as follows: Obtaining zeolite Y spheres with large particle size (ca. 0.5–1 mm) without application of any binder;
2. These particles have pure zeolite Y and partially amorphous SiO_2. But the crystallinity was significantly improved by prolongation of aging time at ambient temperature as discussed in the preceding sections;
3. These particles have hierarchical structures with higher levels of porosity (i.e., secondary meso- and macropores) plus inherent micropores which can alleviate the diffusion limitations originating from zeolite micropores.

2. Materials and Methods

2.1. Materials

Tetramethylammonium hydroxide (TMAOH, 25 wt.% in H_2O), tetraethylammonium hydroxide (TEAOH, 35 wt.% in H_2O), tetrabutylammonium hydroxide (TBAOH, 40 wt.% in

H_2O), silica gel (high purity grade 9385), and AmberliteIRA-900 (with Cl^-) were purchased from Sigma-Aldrich (Taufkirchen, Germany) and sodium aluminate anhydrous (purity 99.5%) was purchased from Riedel-de Haën. MilliQ water was used in all syntheses.

2.2. Synthesis of Zeolite Y

2.2.1. Synthesis in the Absence Organic SDA (Method 1)

Zeolite Y was originally synthesized without using a microporous structure-directing agent (SDA), where inorganic cations such as Na^+ acted as the SDA [16]. Inorganic cations like Na^+ are typically present in aluminum precursors such as sodium aluminate ($NaAlO_2$) and mineralizers like sodium hydroxide (NaOH). In a standard synthesis procedure, 7.55 g of silica gel was mixed with 17.45 g of H_2O and stirred for 1 h. Simultaneously, the aluminum solution was prepared by adding 3.4 g of $NaAlO_2$ and 1.62 g of NaOH to 8 g of H_2O and stirred for 1 h. The aluminum solution was then combined with the silica suspension and stirred for an additional hour. Resin beads were subsequently added to the mixture in a mass ratio of one-twentieth of the total suspension weight [14]. The resulting mixture was transferred into a Teflon bottle, sealed tightly, and aged under static conditions at room temperature for 24 h. It was then subjected to hydrothermal treatment at 100 °C for 72 h. After hydrothermal treatment, the sample was cooled to room temperature, the Teflon bottle was opened, and the product was washed until the pH reached approximately 7–8, followed by overnight drying. To remove the organic phase of the resin, a two-step calcination process was performed using a muffle furnace under static air conditions. The temperature was initially raised from room temperature to 200 °C at a rate of 3 °C/min and held for 6 h at 200 °C. Subsequently, the temperature was increased to 600 °C at a rate of 2 °C/min and maintained for another 6 h at 600 °C. Upon completion of the calcination step, spherical particles—either crystalline zeolite Y, semi-crystalline, or amorphous spheres—were obtained.

2.2.2. Synthesis in the Presence of Organic SDA (Method 2)

As described earlier, the synthesis approach without the use of an organic structure-directing agent (SDA) was unsuccessful in producing highly crystalline zeolite Y within the confined porous environment of a resin template. Therefore, we investigated the effect of organic molecules, such as quaternary ammonium salts, on stabilizing primary SiO_4^{4-} and AlO_4^{5-} species, which are essential for forming the secondary building blocks of zeolite Y (i.e., sodalite and 6-ring units) and further promoting the development of supercages [17].

In a typical synthesis procedure, 2 g of NaOH was dissolved in 15 g of H_2O under mixing for 10 min. Subsequently, 15 g of an aqueous solution of an organic template (tetramethylammonium hydroxide (TMAOH), tetraethylammonium hydroxide (TEAOH), or tetrabutylammonium hydroxide (TBAOH)) was slowly added to the mixture and stirred for 30 min. Next, 1.45 g of $NaAlO_2$ was incorporated, and the mixture was stirred for 1 h. Then, 3 g of silica gel was gradually introduced, and the solution was mixed for an additional 30 min. Finally, the resin template (Amberlite IRA-900-Cl^-) was added at a mass ratio of one-twentieth of the primary mixture, and the suspension was transferred into a Teflon bottle. The bottle was tightly sealed, aged under static conditions at room temperature for 5 to 8 days, and then subjected to hydrothermal treatment using a single- or multi-step temperature program (refer to Section 3.3 of the Results and Discussion). After hydrothermal treatment, the Teflon bottle was allowed to cool to ambient temperature, opened, and the resulting product (a composite of inorganic and organic phases) was collected and washed with water until the pH reached approximately 7–8. Each sample was then dried overnight at 100 °C. The calcination process followed the procedure described previously (refer to Section 2.2.1).

2.3. Characterization of Zeolite Y

X-ray diffraction (XRD) patterns were obtained using a Bruker D-8 Advance Spectrometer with Cu-Kα radiation (λ = 1.5418 Å) operating at 40 kV and 40 mA. Data were collected

over a 2θ range of 5 to 50° with a step size of 0.02° and a scan rate of 1° per minute. Prior to XRD analysis, the zeolite particles were ground into a powder.

The textural porosity was examined using scanning electron microscopy (SEM) on a Philips XL30 ESEM FEG system. Samples were coated with a thin gold layer to ensure conductivity before SEM imaging. Transmission electron microscopy (TEM) images were captured using a CM12 (Philips, Amsterdam, The Netherlands) electron microscope operating at 120 keV. The spherical particles were gently ground into powders, suspended in ethanol, and sonicated for 40 min. One drop of each suspension was placed on a TEM copper grid (400 mesh) with a carbon coating for imaging.

Elemental concentrations in selected samples were measured using X-ray fluorescence (XRF) with a PANalytical Epsilon 3XLE instrument (Malvern Panalytical, Almelo, The Netherlands). For each analysis, 100 mg of a zeolite sample was prepared in a plastic cup with a Mylar film, and elemental quantities were calculated assuming their oxide forms. Fourier Transform Infrared (FTIR) spectroscopy was performed on a Shimadzu IRTracer-100 spectrometer(Shimadzu, Kyoto, Japan) in transmission mode, using a small quantity of zeolite placed on the measurement platform. Nitrogen physisorption isotherms were measured at 196 °C using a Micrometrics ASAP 2420(Micrometrics, Lincolnshire, UK). The BET (Brunauer–Emmet–Teller, BET) and BJH (Barret–Joyner–Halenda, BJH) models were applied to calculate the specific surface area and pore volume, respectively.

3. Results and Discussion

The ion exchange of resin anions (e.g., Cl^-) with zeolitic precursors serves as the driving force for the nucleation of the primary inorganic phase within the pores of the organic resin. Initially, the precipitated phase is amorphous (i.e., during the early stages of the aging process), but with time and precise adjustment of various synthesis parameters, it gradually transforms into a crystalline phase. The organic resin, acting as a template for the nucleation and growth of zeolite Y, is subsequently removed through calcination, leaving behind the zeolite Y structure. This structure exhibits hierarchical porosity, incorporating larger meso- and macropores in addition to the original micropores.

3.1. Effect of the Application of Organic SDA

To investigate the effect of an organic structure-directing agent (SDA) on the crystallization of zeolite Y, we first synthesized a sample using the original synthesis procedure without incorporating any organic molecules as an SDA [16]. The only modification was the addition of resin beads as a shaping template, with an initial suspension/resin mass ratio set at 20:1 (see SEM images in Figure 1 for dimensional and textural properties of resin template) [14]. The XRD analysis results, presented in Figure 2a, show a semi-crystalline phase with characteristic peaks of zeolite Y for the spherical particles obtained through the hard templating technique. For comparison, the crystalline powder obtained from the same synthesis batch is shown in Figure 2b. The observed amorphization of the precipitated phase on the resin surface and the absence of organic SDA are likely due to the competitive rates of precursor deposition within the resin's porous structure. This discrepancy limits the ordered alignment of precursors. Additionally, the resin template's chemistry differs from that of the initial suspension and the bulk of the formed zeolite, while its porous structure partially imposes steric hindrance, affecting the movement and alignment of the precursors in an orderly fashion.

To address the issue of amorphization within the resin pores, we utilized various organic molecules as micropore structure-directing agents (SDAs) to encapsulate the inorganic zeolite species through the formation of organic cations. These organic–inorganic complexes were expected to promote the formation of primary zeolite Y nuclei, leading to the sequential development of secondary building units and the further propagation of an ordered lattice structure in subsequent steps.

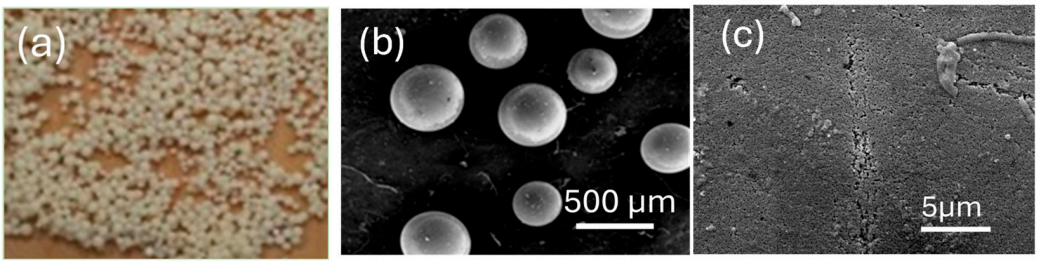

Figure 1. (**a**) Spherical appearance of Amberlite IRA900 (0.5–1 mm), and (**b**) the SEM image of resin beads as macroscopic hard templates, (**c**) the SEM image of spherical resin surface possessing large meso- and macropores.

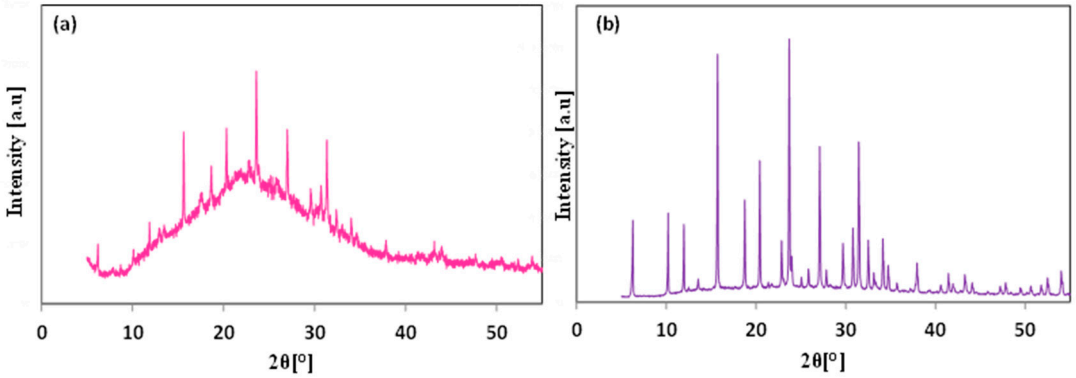

Figure 2. The XRD pattern of (**a**) zeolite Y spheres synthesized in the absence of organic SDA (semicrystalline phase); (**b**) crystalline zeolite Y powder synthesized with the same synthesis route.

In different experimental batches, we examined the influence of organic ammonium salts such as tetramethylammonium hydroxide (TMAOH), tetraethylammonium hydroxide (TEAOH), and tetrabutylammonium hydroxide (TBAOH) on the crystallization of zeolite Y using synthesis method 2 (see Section 2.2.2). In all experiments, the aging duration was fixed at 5 days, and crystallization was carried out under a single-step temperature program at 100 °C for 72 h. The XRD patterns of the samples are presented in Figure 3. The addition of TEAOH or TBAOH showed lower affinity for interacting with inorganic precursors to form the characteristic pores and cages of zeolite Y, resulting in a significant amount of amorphous phase as a competing product (Figure 3a,b). These patterns indicate that the zeolite Y framework was not well-formed under these synthesis conditions with TEAOH and TBAOH as SDAs. In contrast, TMAOH resulted in the highest degree of crystallinity for the zeolite Y beads under the same conditions, with significantly reduced amorphous phases, as confirmed by XRD analysis (Figure 3c) [18]. The textural properties of the obtained spherical particles have been shown by SEM imaging (Figure 4a–c). The spherical geometry of obtained zeolite Y particles (particle diameter <1mm) can be seen with naked eyes (Figure 4d). The hierarchical structure of zeolite Y beads have been also proved by N_2 physisorption (see Figure 5a) in which a hysteresis loop appeared at ca. $p/p0 > 0.9$ indicating that large mesopores and macropores are present inside the material. The pore size distribution is presented in Figure 5b, indicating the presence of large mesopores with a pore width < 40 nm and pore volume of 0.5 cm^3/g.

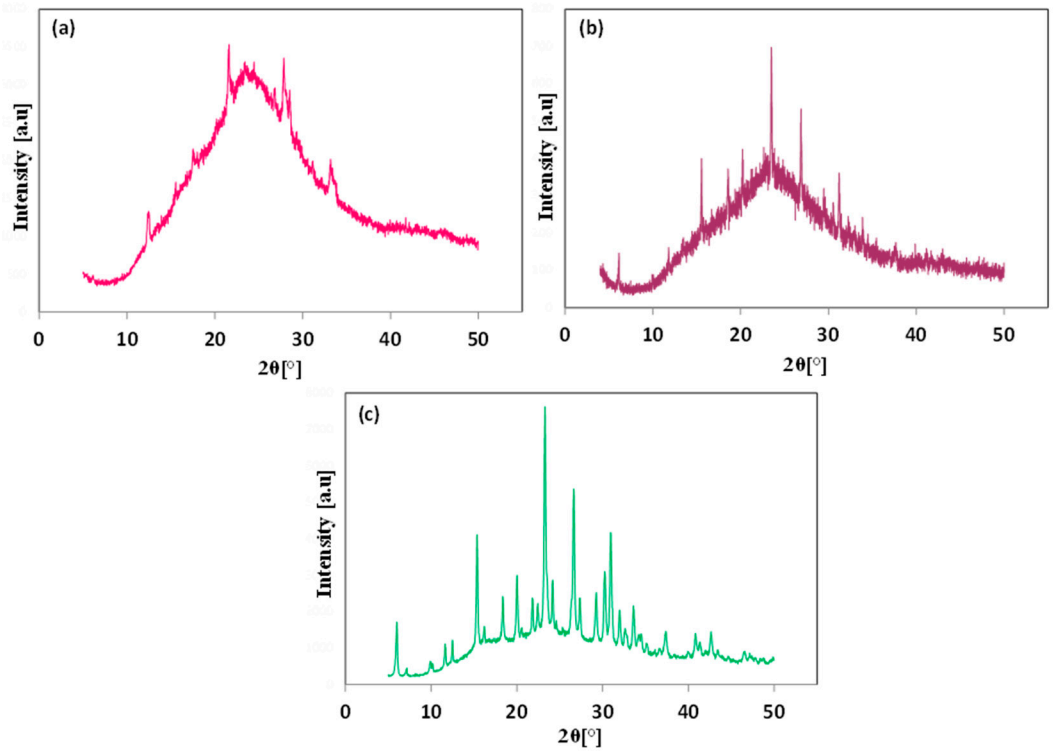

Figure 3. The XRD pattern of (**a**) sample synthesized using TEAOH; (**b**) sample synthesized using TBAOH; and (**c**) sample synthesized using TMAOH. All samples were aged for 5 days.

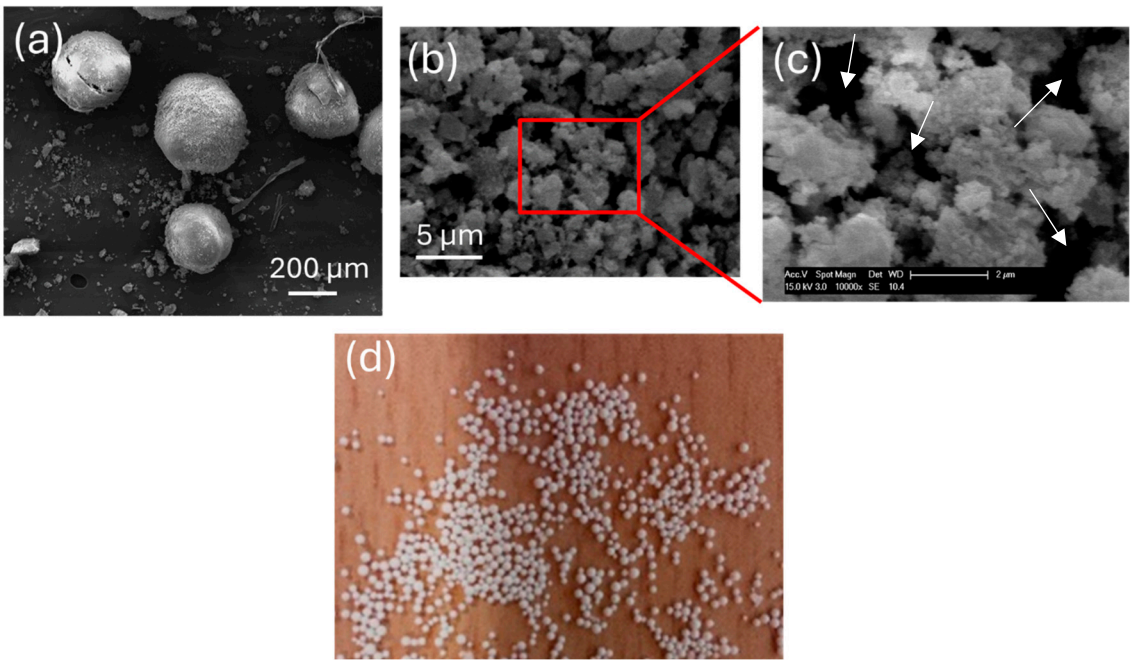

Figure 4. The SEM image of (**a**) spherically shaped zeolite Y, (**b**,**c**) spherical zeolite Y surface morphology and textural porosities, (**d**) zeolite Y particles obtained after calcination.

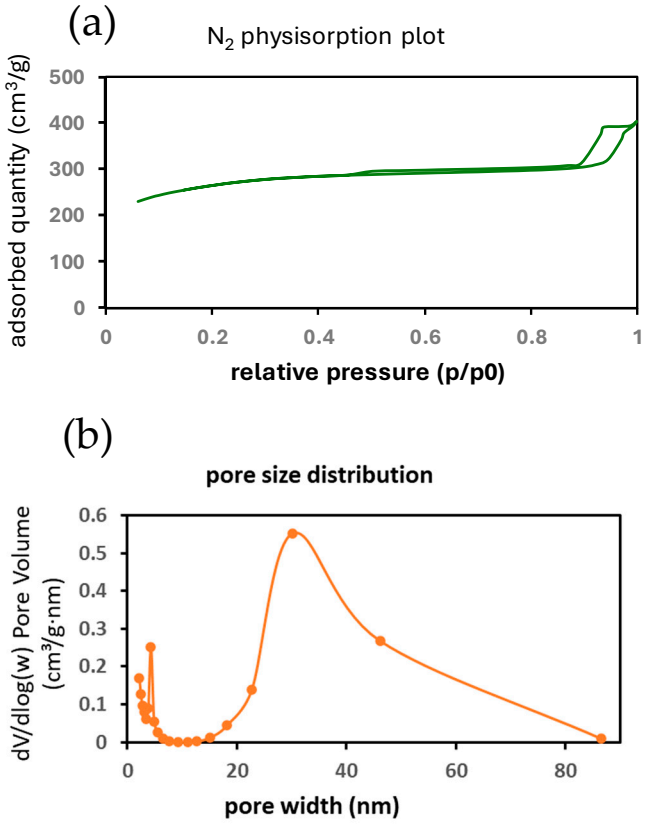

Figure 5. (**a**) N_2 physisorption plot and (**b**) pore size distribution of spherical zeolite Y, based on adsorption branch.

It is important to note that the use of structure-directing agents (SDAs) is not restricted to a specific zeolite topology [17]. In fact, multiple topologies can be synthesized using the same SDA, with the primary variation being the boundary conditions; beyond these conditions, the formation of the specific zeolite type is not feasible. Additionally, the co-templating approach allows for the synthesis of various zeolite frameworks by employing two or more different SDAs, simultaneously [17]. Based on the results obtained, TMAOH was selected as the most suitable organic SDA for the crystallization of zeolite Y particles. The next objective was to optimize and enhance the crystallization process for zeolite Y further. The TEM image of the sample synthesized using TMAOH, shown in Figure 6, confirms the successful formation of zeolite Y, as the particles exhibit a polyhedral morphology—a characteristic feature of zeolite Y [19].

To further investigate the structural properties of the zeolite Y beads synthesized using TMAOH, the FTIR spectrum of this sample was obtained and compared with that of fully crystalline zeolite Y powder (refer to Figure 1b for the XRD pattern). In the FTIR spectra (400–1400 cm^{-1}), both samples exhibited transmission bands corresponding to the symmetric and asymmetric stretching of T-O-T bonds at approximately 750–790 cm^{-1} and 990–1010 cm^{-1}, respectively, where "T" denotes either Si or Al atoms. As shown in the FTIR spectra (Figure 7a,b), the spherical zeolite Y particles exhibited a shift in the characteristic peaks towards lower wavenumbers compared to the reference crystalline Y powder. This shift is likely due to differences in the chemical composition between the two samples [20]. This finding is further supported by XRF measurements, which are discussed in the following section.

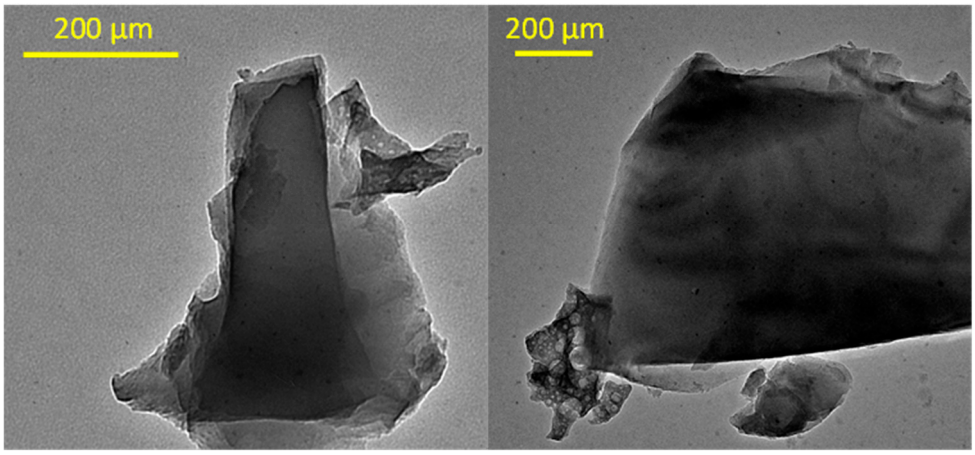

Figure 6. The TEM images of particles of zeolite Y spheres which were prepared by application of TMAOH (microporous structure directing agent) in the synthesis mixture. These particles which were obtained by sonication of zeolite Y beads in ethanol after grinding represent the common crystalline structure of zeolite Y.

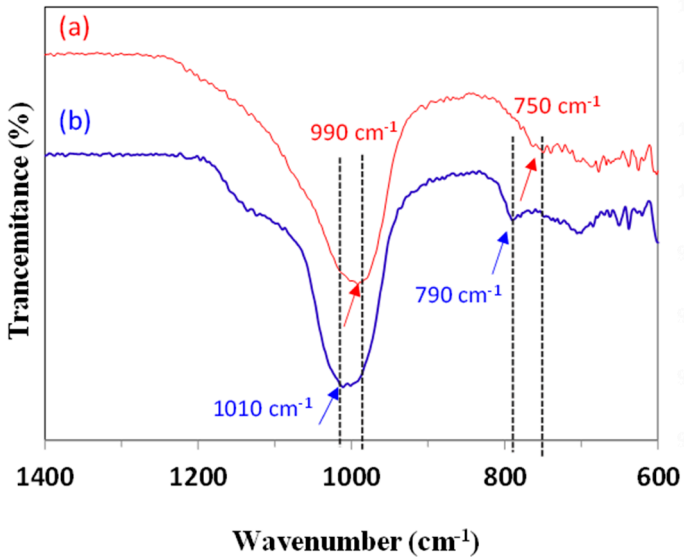

Figure 7. The FTIR analysis of (**a**) crystalline zeolite Y spheres prepared by application of TMAOH in the synthesis mixture, (**b**) crystalline zeolite Y powder prepared in the absence of any organic SDA (as a reference material).

We analyzed the effect of TMAOH on the Si/Al ratio of zeolite Y using X-ray fluorescence (XRF) analysis. Interestingly, the zeolite Y beads synthesized in the presence of TMAOH exhibited a Si/Al molar ratio of 1.7, while the zeolite Y beads prepared without the structure-directing agent (SDA) displayed a higher Si/Al molar ratio of 8.8. This finding is consistent with the formation of an amorphous SiO_2 phase in the latter sample, as indicated by a broad peak between 2θ = 15° and 35° in its XRD pattern, which is characteristic of amorphous SiO_2 (see Figures 2a and 3a,b) [14]. Furthermore, we measured the Si/Al ratio of the reference crystalline zeolite Y powder synthesized in the absence of any organic SDA, which yielded a Si/Al molar ratio of 2.9. These results confirm that the presence of the organic SDA can significantly alter the chemical composition of the zeolite, as organic cations may compete with Al^{3+} and Na^{+} to balance the total negative charge within the framework [17]. Additionally, we investigated the anion-exchange capability of the resin template after substituting Cl^{-} with I^{-} using a straightforward protocol involving KI aqueous solution and ion exchange under mild conditions (stirring for 4 h at 65 °C) [15].

However, this sample demonstrated poor anion-exchange ability, adversely affecting the crystallization process, as the final inorganic product was entirely amorphous (see Figure 8). This result underscores that iodide is a notably weaker anion for exchange with zeolite inorganic precursors compared to chloride, likely due to its larger size, steric hindrance, and consequently reduced reactivity in the reaction medium.

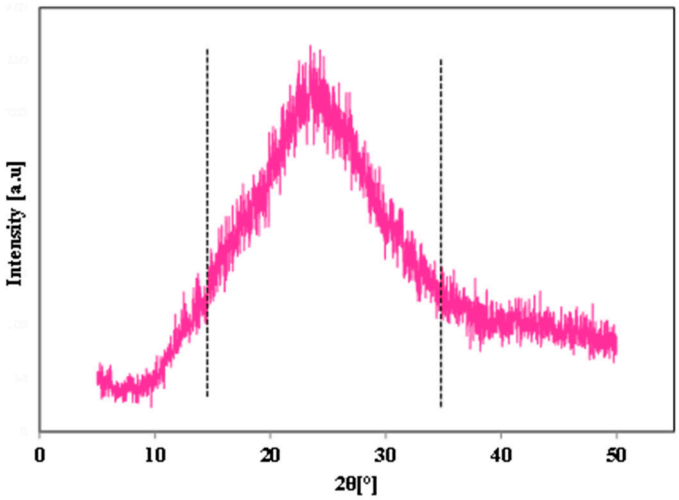

Figure 8. The XRD pattern of the sample synthesized using ion-exchanged resin beads with KI solution.

3.2. Effect of Aging Time

The aging period exhibits slower kinetic rates compared to hydrothermal treatment, which occurs at elevated temperatures and consequently accelerates both crystallization and amorphization rates. To enhance the crystallinity of zeolite Y regarding its crystallization nature, it is essential to prolong the aging time, as this likely promotes the induction of nuclei and the stabilization of inorganic precursors within the structural framework of zeolite Y in the presence of the resin template and TMAOH. It underlines that for reaching an ordered arrangement of atoms instead of their random movement, for zeolite Y, the primary zeolite Y suspension should be aged for longer time which implicitly is related to the control of crystallization kinetics upon the time. Therefore, we investigated a range of aging times from 5 to 8 days at ambient temperature. The XRD pattern of zeolite Y aged for 5 days is presented in Figure 3c (see above). The results illustrating the effects of prolonged aging time are depicted in Figure 9a,b with 6 and 7 aging days at ambient temperature, respectively. As shown, extending the aging time significantly improves the crystallinity of the zeolite Y beads. This may be ascribed to improving the transformation of amorphous phase to zeolite Y crystallites at the initial stage of crystalline phase formation, based on our empirical observation.

This observation becomes more evident when all spectra are analyzed in a overlaid curve (Figure 10), where the peak/noise ratio gradually decreases with increasing aging time. However, upon extending the aging time to 8 days, peaks corresponding to other zeolitic phases, such as zeolite P and A, begin to appear gradually [21]. The detected peaks for zeolite P and A are indicated by red arrows in Figure 9c. Based on these results, we conclude that while prolonging the aging time in the presence of the resin shaping template can enhance crystallinity, it also has limitations. Under these crystallization conditions, extending the aging time does not guarantee the formation of pure zeolite Y particles, as some other amorphous or crystalline competitive phases may form concurrently.

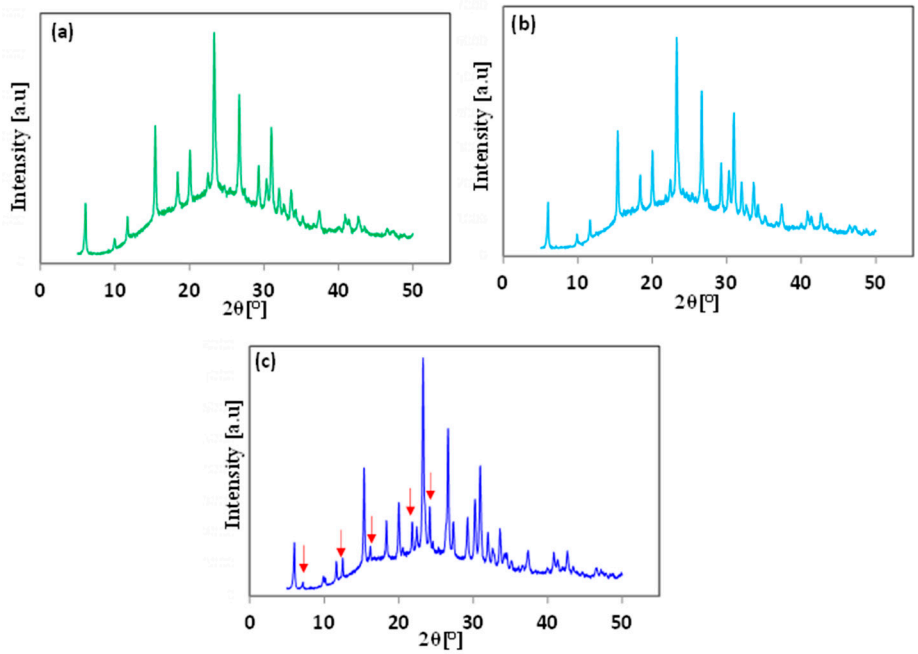

Figure 9. The XRD pattern of zeolite Y beads aged for (**a**) 6 days, (**b**) 7 days, and (**c**) 8 days using hydrothermal treatment using single temperature program at 100 °C for 72 h. The red arrows indicate the peaks belonging to zeolite *p* and zeolite L.

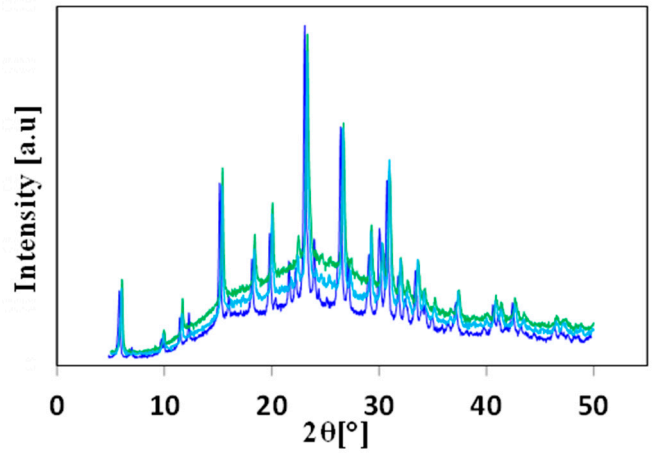

Figure 10. The stacking XRD spectra of aged zeolites beads (green: 6 days, light blue: 7 days, and dark blue: 8 days).

Furthermore, the zeolite Y beads obtained after aging for 8 days exhibited a significantly larger particle size, as visualized by scanning electron microscopy (SEM) in Figure 11b, compared to those aged for 5 days (Figure 11a). This observation aligns with previously reported findings in the literature regarding the effects of aging time [22–24]. SEM imaging clearly indicates that crystallization can be enhanced with prolonged aging time. After 5 days of aging, the sample particles displayed irregular morphologies, suggesting that the polyhedra were covered by an amorphous phase (Figure 11a). In contrast, after 8 days of aging (Figure 11b), the sample particles exhibited notably cleaner and more distinct polyhedron morphologies. However, as previously mentioned, this latter sample also contained other crystalline co-phases, leading to the formation of an inorganic composite rather than a pure zeolite Y phase.

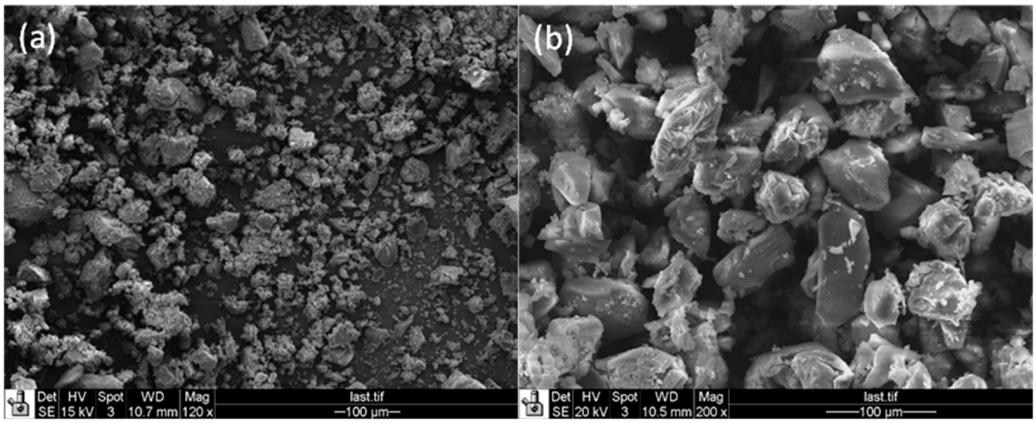

Figure 11. The SEM image of the surface of the samples aged for (**a**) 5 days and (**b**) 8 days. Scale bar is 100 µm in both images [17].

3.3. Effect of Hydrothermal Temperature Program

Based on the aforementioned behavioral characteristics observed in zeolite Y spheres resulting from various synthetic modifications, the sample aged for 7 days with TMAOH as the organic structure-directing agent was identified as the most crystalline sample. To further investigate the effect of a multi-step temperature program during the hydrothermal treatment, a new sample was prepared under the same synthesis conditions. However, the hydrothermal crystallization process was executed using a stepwise temperature program. Initially, the sample was heated from ambient temperature to 50 °C at a ramp rate of 3 °C/min and held at this temperature for 48 h. Subsequently, the temperature was increased to 100 °C at a ramp rate of 2 °C/min and maintained at this temperature for an additional 30 h in an oven under static air conditions. The subsequent procedures, including washing, drying, and calcination, were conducted as described in the previous synthesis trials (see Section 2.2). The results indicated that the multi-step heating approach during hydrothermal crystallization was more effective in achieving higher degrees of crystallinity (Figure 12). This enhancement is likely attributed to the reduced kinetics for the formation of competitive phases, thereby allowing for better control over the purity of the zeolite Y phase.

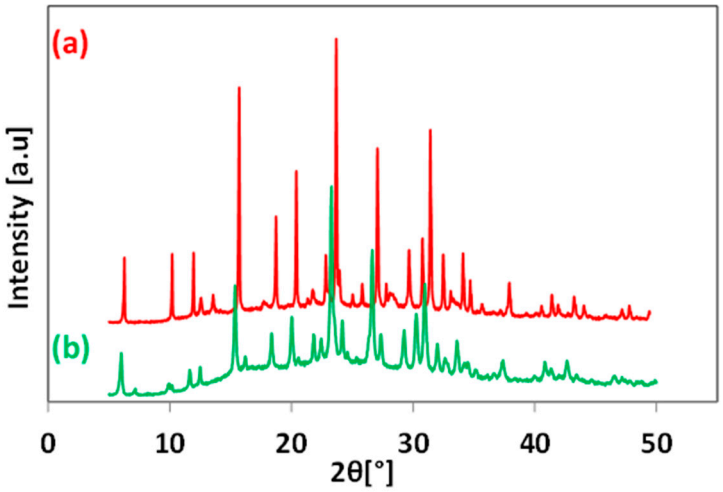

Figure 12. The XRD pattern of zeolite Y sample aged for 7 days in the presence of TMAOH, and resin template (**a**) crystallized using stepwise heating program, (**b**) crystallized using single heating program.

Indeed, when a one-step treatment cannot result in the desired degree of crystallinity, a multi-step temperature program may assist with better control of the rate of crystallization, as was the case for zeolite Y, particularly, in this study. It can also suppress the possible thermal shock of the final target temperature (e.g., 100 °C). When we increase the hydrothermal temperature in a stepwise protocol, we allow better control of amorphous phase transformation to the crystalline phase.

The samples after hydrothermal treatment, washing, and drying were subjected to 600 °C heating during the calcination step for complete removal of the resin template and microporous organic structure-directing agent. Any temperature below this (e.g., 550 °C) resulted in non-complete removal of resin templates, and partially gray spherical zeolitic particles were obtained at the end of calcination, highlighting that the organic compounds were not completely removed from the porous structure of zeolite beads. So, applying higher temperature (i.e., 600 °C) became useful to get rid of all remaining carbon species from the porous zeolite particles.

4. Conclusions

In this study, we examined the influence of synthetic parameters on the formation of spherically shaped zeolite Y with hierarchical porosity using a hard templating technique. These structured particles represent suitable candidates for research in the fields of catalysis and adsorption, including kinetic studies, coke formation, and deactivation mechanisms. Specifically, they can serve as catalysts or sorbents in laboratory-scale fixed-bed reactors. Our findings indicate that the chemical properties of the resin template can significantly affect the crystallization process. To achieve an almost pure zeolite Y phase on the surface of the resin template, the synthesis parameters must be constrained within a narrower range compared to conventional methods for synthesizing zeolite Y powder. We successfully obtained nearly pure zeolite Y beads by extending the aging time to 7 days, implementing a multi-step temperature program during hydrothermal crystallization, and utilizing an organic structure-directing agent (SDA), with TMAOH identified as an effective organic molecule under the selected synthesis conditions. Furthermore, the application of organic SDAs may be extended to other low Si/Al ratio zeolites, such as zeolite A and zeolite X [25–28]. Future research could explore the effects of other organic molecules, such as branched or linear amines, on the crystallinity of the final product during the synthesis of these zeolitic particles. These functional materials have been used as catalysts for anisole acylation reactions [14] and as adsorbents for selective CO_2 adsorption [29], highlighting the capability of binder-free zeolite Y particles in different application fields.

Author Contributions: Conceptualization, Z.A.P. and Y.A.A.; methodology, M.E.H.E.N.; software, E.A.Z.; validation, K.O.S., P.H.M.V.S. and Y.A.A.; formal analysis, K.O.S.; investigation, Z.A.P.; resources, E.A.Z.; data curation, Z.A.P.; writing—original draft preparation, K.O.S.; writing—review and editing, M.E.H.E.N.; visualization, Z.A.P.; supervision, K.O.S. and Y.A.A.; project administration, K.O.S.; funding acquisition, K.O.S. All authors have read and agreed to the published version of the manuscript.

Funding: This research received no external funding.

Data Availability Statement: The original contributions presented in the study are included in the article, further inquiries can be directed to the corresponding authors.

Acknowledgments: Khaled O. Sebakhy thanks the Laboratory for Chemical Technology (LCT), University of Ghent.

Conflicts of Interest: The authors declare no conflicts of interest.

References

1. Rhodes, C.J. Properties, and applications of zeolites. *Sci. Prog.* **2010**, *93*, 223–284. [CrossRef]
2. Nesic, A.; Meseldzija, S.; Cabrera-Barjas, G.; Onjia, A. Novel biocomposite films based on high methoxyl pectin reinforced with zeolite Y for food packaging applications. *Foods* **2022**, *11*, 360. [CrossRef]

3. Zeigermann, P.; Kärger, J.; Valiullin, R. Diffusion in microporous materials with embedded mesoporosities. *Microporous Mesoporous Mater.* **2013**, *178*, 84–89. [CrossRef]
4. Peng, P.; Gao, X.H.; Yan, Z.F.; Mintova, S. Diffusion and catalyst efficiency in hierarchical zeolite catalysts. *Natl. Sci. Rev.* **2020**, *7*, 1726–1742. [CrossRef]
5. Zhang, K.; Ostraat, M.L. Innovations in hierarchical zeolite synthesis. *Catal. Today* **2016**, *264*, 3–15. [CrossRef]
6. Liu, Z.; Hua, Y.; Wang, J.; Dong, X.; Tian, Q.; Han, Y. Recent progress in the direct synthesis of hierarchical zeolites: Synthetic strategies and characterization methods. *Mater. Chem. Front.* **2017**, *1*, 2195–2212. [CrossRef]
7. Maghfirah, A.; Ilmi, M.M.; Fajar, A.T.N.; Kadja, G.T.M. A review on the green synthesis of hierarchically porous zeolite. *Mater. Today Chem.* **2020**, *17*, 100348. [CrossRef]
8. Asgar Pour, Z.; Abduljawad, M.M.; Alassmy, Y.A.; Cardon, L.; Van Steenberge, P.H.; Sebakhy, K.O. A Comparative review of binder-containing extrusion and alternative shaping techniques for structuring of zeolites into different geometrical bodies. *Catalysts* **2023**, *13*, 656. [CrossRef]
9. Yue, M.B.; Sun, M.N.; Xie, F.; Ren, D.D. Dry-gel synthesis of hierarchical TS-1 zeolite by using P123 and polyurethane foam as template. *Microporous Mesoporous Mater.* **2014**, *183*, 177–184. [CrossRef]
10. Dakhchoune, M.; Duan, X.; Villalobos, L.F.; Avalos, C.E.; Agrawal, K.V. Hydrogen-sieving zeolitic films by coating zeolite nanosheets on porous polymeric support. *J. Membr. Sci.* **2023**, *672*, 121454. [CrossRef]
11. Tosheva, L.; Valtchev, V.; Sterte, J. Silicalite-1 containing microspheres prepared using shape-directing macro-templates. *Microporous Mesoporous Mater.* **2000**, *35–36*, 621–629. [CrossRef]
12. Tosheva, L.; Sterte, J. ZSM-5 spheres prepared by resin templating. *Stud. Surf. Sci. Catal.* **2002**, *142*, 183–190. [CrossRef]
13. Tosheva, L.; Mihailova, B.; Valtchev, V.; Sterte, J. Zeolite beta spheres. *Microporous Mesoporous Mater.* **2001**, *48*, 31–37. [CrossRef]
14. Asgar Pour, Z.; Koelewijn, R.; El Hariri El Nokab, M.; van der Wel, P.C.; Sebakhy, K.O.; Pescarmona, P.P. Binder-free zeolite beta beads with hierarchical porosity: Synthesis and application as heterogeneous catalysts for anisole acylation. *ChemCatChem* **2022**, *14*, e202200518. [CrossRef]
15. Alassmy, Y.A.; Asgar Pour, Z.; Pescarmona, P.P. Efficient and easily reusable metal-free heterogeneous catalyst beads for the conversion of CO_2 into cyclic carbonates in the presence of water as hydrogen-bond donor. *ACS Sustain. Chem. Eng.* **2020**, *8*, 7993–8003. [CrossRef]
16. Breck, D.W. Crystalline Zeolite Y. U.S. Patent 3,130,007, 21 April 1964.
17. Asgar Pour, Z.; Sebakhy, K.O. A review on the effects of organic structure-directing agents on the hydrothermal synthesis and physicochemical properties of zeolites. *Chemistry* **2022**, *4*, 431–446. [CrossRef]
18. Holmberg, B.A.; Wang, H.; Norbeck, J.M.; Yan, Y. Controlling size and yield of zeolite Y nanocrystals using tetramethylammonium bromide. *Microporous Mesoporous Mater.* **2003**, *59*, 13–28. [CrossRef]
19. Susanti, I.; Widiastuti, N. Activation of zeolite-Y templated carbon with KOH to enhance the CO_2 adsorption capacity. *Malays. J. Fundam. Appl. Sci.* **2019**, *15*, 240–253.
20. Król, M.; Koleżyński, A.; Mozgawa, W. Vibrational spectra of zeolite Y as a function of ion exchange. *Molecules* **2021**, *26*, 342. [CrossRef]
21. Belaabed, R.; Elknidri, H.; Elkhalfaouy, R.; Abdellah; Addaou; Laajab, A.; Lahsini, A. Zeolite Y synthesis without organic template: The effect of synthesis parameters. *J. Mater. Environ. Sci.* **2017**, *8*, 3550–3555.
22. Bo, W.; Hongzhu, M. Factors affecting the synthesis of microsized NaY zeolite. *Microporous Mesoporous Mater.* **1998**, *25*, 131–136. [CrossRef]
23. Ginting, S.B.; Yulia, Y.; Wardono, H.; Hanif, M.; Iryani, D.A. Synthesis and characterization of zeolite lynde type A (LTA): Effect of aging time. *J. Phys. Conf. Ser.* **2019**, *1376*, 1–7. [CrossRef]
24. Faghihian, H.; Godazandeha, N. Synthesis of nano crystalline zeolite Y from bentonite. *J. Porous Mater.* **2009**, *16*, 331–335. [CrossRef]
25. Sebakhy, K.O.; Vitale, G.; Pereira-Almao, P. Dispersed Ni-doped aegirine nanocatalysts for the selective hydrogenation of olefinic molecules. *ACS Appl. Nano Mater* **2018**, *1*, 6269–6280. [CrossRef]
26. Sebakhy, K.O.; Vitale, G.; Pereira-Almao, P. Production of highly dispersed Ni within nickel silicate materials with the MFI structure for the selective hydrogenation of olefins. *Ind. Eng. Chem. Res.* **2019**, *58*, 8597–8611. [CrossRef]
27. Asgar Pour, Z.; Alassmy, Y.; Sebakhy, K.O. A survey on zeolite synthesis and the crystallization process: Mechanism of nucleation and growth steps. *Crystals* **2023**, *13*, 959. [CrossRef]
28. Asgar Pour, Z.; Abduljawad, M.M.; Alassmy, Y.; Alnafisah, M.S.; El Hariri El Nokab, M.; Van Steenberge, P.H.M.; Sebakhy, K.O. Synergistic catalytic effects of alloys of noble metal nanoparticles supported on two different supports: Crystalline zeolite Sn-Beta and carbon nanotubes for glycerol conversion to methyl lactate. *Catalysts* **2023**, *13*, 1486. [CrossRef]
29. Boer, D.G.; Asgar Pour, Z.; Langerak, J.; Bakker, B.; Pescarmona, P. P Binderless Faujasite beads with hierarchical porosity for selective CO_2 adsorption for biogas upgrading. *Molecules* **2023**, *28*, 2198. [CrossRef]